

Spectrum and Morphology of the Ultra-High-Energy Source LHAASO J2018+3651

Huicai Li ^{a,b} Chao Hou, ^{a,b} B. Theodore Zhang, ^{a,b} Xiao Zhang, ^c Yang Chen, ^d Ping Zhou, ^d Jun Fang^e and On behalf of LHAASO collaboration

^a*Key Laboratory of Particle Astrophysics & Experimental Physics Division & Computing Center, Institute of High Energy Physics, Chinese Academy of Sciences, 100049 Beijing, China*

^b*Tianfu Cosmic Ray Research Center, 610000 Chengdu, Sichuan, China*

^c*School of Physics and Technology, Nanjing Normal University, 210023 Nanjing, Jiangsu, China*

^d*School of Astronomy and Space Science, Nanjing University, 210023 Nanjing, Jiangsu, China*

^e*School of Physics and Astronomy, Yunnan University, 650091 Kunming, Yunnan, China*

The LHAASO J2018+3651 region is one of the brightest sources in the sky at TeV energies. Photons with energies up to 0.27 PeV from this region have been detected with the Large High Altitude Air Shower Observatory (LHAASO) and here we present a detailed study of this region using more data from LHAASO. This analysis resolves the region into six sources: LHAASO J2018+3641, LHAASO J2019+3649, LHAASO J2021+3657, LHAASO J2016+3712, LHAASO J2013+3610 and LHAASO J2028+3655. An investigation of the morphology and spectrum for LHAASO J2018+3641, LHAASO J2019+3649 and LHAASO J2021+3657 are the focus and we find that the spectrum above TeV deviates significantly from a single power-law, and is best described by a power-law with exponential cutoff. The three sources may be associated with PSR J2021+3651 and its X-ray pulsar wind nebula. Additionally, LHAASO J2016+3712 is tentatively associated with the evolved supernova remnant CTB 87.

39th International Cosmic Ray Conference (ICRC2025)
15–24 July 2025
Geneva, Switzerland

 **ICRC 2025**
The Astroparticle Physics Conference
Geneva July 15–24, 2025

1. Introduction

The LHAASO J2018+3651 region is one of the brightest sources in the sky at TeV energies, which was first observed by the Milagro for MGRO J2019+37[1]. Milagro measured its flux to be about 80% of the Crab Nebula flux at 20 TeV and showed an extent of $\sim 0.75^\circ$ [2]. Deep observations of this region by VERITAS resolved it into two sources: VER J2019+368 and VER J2016+371 [6]. VER J2019+368 is a brighter extended source. More tests provide statistically significant evidence that the emission is due to two independent sources (the potential sources VER J2018+367* and VER J2020+368*), the two sources are still candidates and may be related, meanwhile the origin of the emission remained unknown [3]. VER J2016+371 is the other source, which is a point-like source to VERITAS. It was suggested that the most likely counterpart of VER J2016+371 is a Pulsar Wind Nebula (PWN) in the Supernova Remnant (SNR) CTB 87 because of the co-location of the TeV γ -ray and X-ray emission as well as the luminosity in those energy ranges.

Moreover, HAWC identified a source HAWC J2019+368 associated with VER J2019+368, and it has significant VHE γ -ray emission above 56 TeV ([4]). LHAASO identified a source LHAASO J2018+3651, reported that γ -rays with energies up to 0.27 PeV were detected from the source, which is associated with VER J2019+368 [8]. The observation with the Tibet air shower array detected γ -rays of TASG J2019+368 have energies up to 200 TeV with a spectrum that can be fitted with an exponential cutoff with an index of 1.6 ± 0.5 and a cutoff energy of 44 ± 21 TeV [7].

Within the region encompassing LHAASO J2018+3651, a fascinating amalgamation of astronomical phenomena is observed, including several supernova remnants (SNRs), HII regions, Wolf-Rayet (WR) stars, high-energy γ -ray (> 100 MeV) sources, and the hard X-ray transient IGR J20188+3647 (17–30 keV) [2, 8, 16]. A young energetic radio and γ -ray pulsar, PSR J2021+3651 [11, 15] and its nebula, PWN G75.1+0.2, are also in the vicinity. PSR J2021+3651 has a period (P) of 104 ms, spin-down luminosity (\dot{E}) of 3.4×10^{36} erg s $^{-1}$ and a characteristic age (τ_c) of 17.2 kyr [15]. Observations with Chandra, Suzaku, and XMM-Newton detected a nebula named PWN G75.2+0.1 around PSR J2021+3651 [12]. Based on a one-zone time-dependent model for multiband nonthermal emission from PWNe, [9] indicated that the pulsar could provide enough energy into the PWN G75.2+0.1 to produce the 100 TeV gamma ray source. Assuming a power-law distribution for the electrons/positrons injected into the nebula, the obtained PWN spectral energy distribution is in general agreement with the fluxes detected by the VLA, Suzaku+XMM-Newton, and HAWC [9, 12].

We will examine the morphology and spectrum of LHAASO J2018+3651 in this work, which combines and extends the prior analyses presented in [8]. The high-energy sensitivity will enable us to probe spectral features such as the existence of a spectral softening beyond the VERITAS and HAWC energy range, which would be expected if the TeV emission originates from inverse Compton (IC) scattering. Significant softening in the spectrum favors a leptonic scenario, because of the suppression of the γ -ray emission due to Klein-Nishina (KN) effects [14].

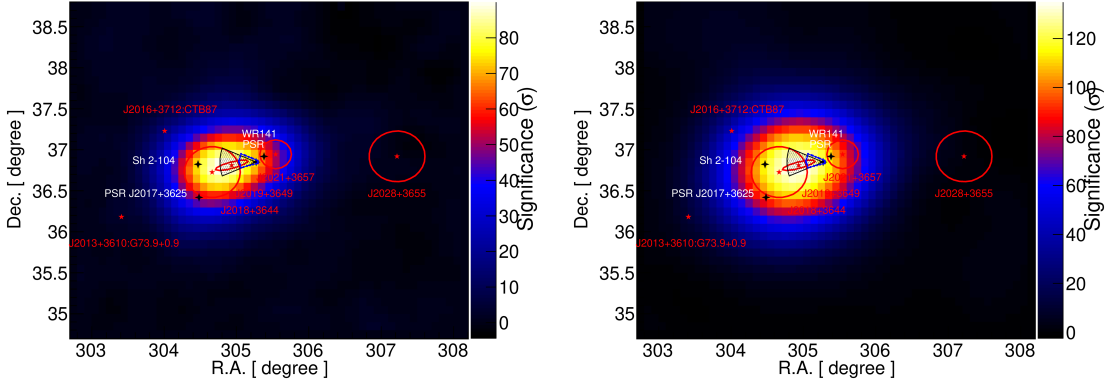


Figure 1: The LHAASO exposure significance map of the observations used in this analysis (Left: LHAASO-WCDA; Right: LHAASO-KM2A). The X-ray radiation is represented by a blue fan-shaped region, and the radio radiation is represented by a black fan-shaped region.

2. Observations

2.1 LHAASO data analysis

LHAASO, a versatile extensive air shower (EAS) array, is purpose-built for investigating cosmic rays (CRs) and gamma rays across an energy spectrum spanning from sub-TeV to over 1 PeV. This advanced facility integrates three detector systems: the 1.3 km² Kilometer-Square Array (KM2A), which offers unprecedented gamma-ray detection sensitivity above 20 TeV; the 78,000 m² Water Cherenkov Detector Array (WCDA), engineered for TeV gamma-ray observations; and the Wide Field-of-view Cherenkov Telescopes Array (WFCTA), specialized in cosmic ray physics research.

For this study, we employed the full-array setup, with WCDA data collected from March 5th, 2021, to July 31st, 2024 (1136.2 days effective live time) and KM2A data from July 20th, 2021, to July 31st, 2024 (1064.9 days). The number of fired hits (N_{hit}) was selected as the primary energy estimator for WCDA [5], with events binned into seven segments: [30, 60), [60, 100), [100, 200), [200, 300), [300, 500), [500, 800), and ≥ 800 . KM2A events were log-binned with a 0.2 energy width. The cosmic ray background was estimated using the direct integral method [10]. The celestial region (RA 0°–360°, Dec –20°–80°) was divided into 0.1°×0.1° pixels, where detected events and estimated background were filled for binned maximum likelihood analysis based on the forward folding method. The significance of the target source was calculated via the test statistic (TS): $TS = -2(\ln \mathcal{L}_b - \ln \mathcal{L}_{s+b})$, where \mathcal{L}_b and \mathcal{L}_{s+b} denote likelihoods for the background-only and signal+background models, respectively. Assuming a power-law (PL) spectrum with pivot energy $E_0=10$ TeV, the forward folding method was used to derive the gamma-ray spectral energy distribution (SED), with spectrum parameters obtained via maximum likelihood fitting.

2.2 Spectral and Morphological

As illustrated in Figure 1, the emission near the center of the region of interest (ROI) dominates this area. To better fit the data, we employed an alternative elliptical Gaussian shape model; however,

Table 1: Description of model parameters assuming sources have an exponentially cutoff power law spectrum. $\phi_{10\text{ TeV}}$ is the flux normalization at 10 TeV in units of $\text{TeV}^{-1} \text{ cm}^{-2} \text{ s}^{-1}$. Reported uncertainties are statistical. For the DGE, a log-parabola (LP) function is employed for fitting.

Source Name	RA and DEC [°]	Spectral Parameters	Morphology (σ)
LHAASO J2018+3644	304.67 ± 0.013	$\Gamma = 1.59 \pm 0.04$	$0.254^\circ \pm 0.012^\circ$
	36.73 ± 0.01	$E_{\text{cut}} = 18.85 \pm 0.56 \text{ TeV}$	
LHAASO J2019+3649	304.92 ± 0.02	$\Gamma = 1.33 \pm 0.02$	$0.029^\circ \pm 0.004^\circ$
	36.81 ± 0.01	$E_{\text{cut}} = 40.44 \pm 1.60 \text{ TeV}$	$0.218^\circ \pm 0.023^\circ$ $100.700^\circ \pm 2.172^\circ$
LHAASO J2021+3657	305.56 ± 0.03	$\Gamma = 1.89 \pm 0.08$	$0.170^\circ \pm 0.018^\circ$
	36.95 ± 0.02	$E_{\text{cut}} = 31.52 \pm 3.25 \text{ TeV}$	
Background	–	$\Gamma = 2.752 \pm 0.015$	Dust Model
	–	$\beta = 0.076 \pm 0.009$	

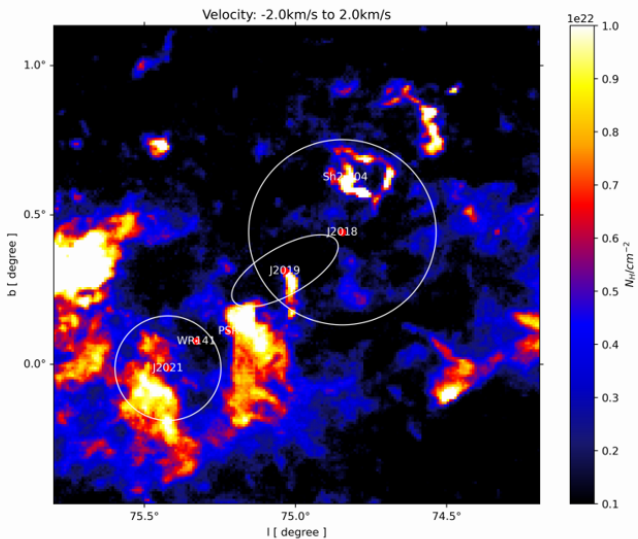


Figure 2: The gas column density near this region derived from ^{12}CO line observations.

the results did not yield convincing evidence to support its applicability. Three source candidates were identified: LHAASO J2018+3641, LHAASO J2019+3649, and LHAASO J2021+3657. All three sources exhibit local significance exceeding 20σ , and their spectra are well-described by a power-law function with an exponential cutoff, given by

$$\frac{dN}{dE} \propto \left(\frac{E}{E_0} \right)^{-\Gamma} \exp \left(-\frac{E}{E_{\text{cut}}} \right), \quad (1)$$

where Γ is the spectral index and E_{cut} is the cutoff energy, Γ is the photon index of the spectrum. For Energy-dependent morphology, the measured size exhibits large uncertainties, and no significant variation is observed with increasing energy.

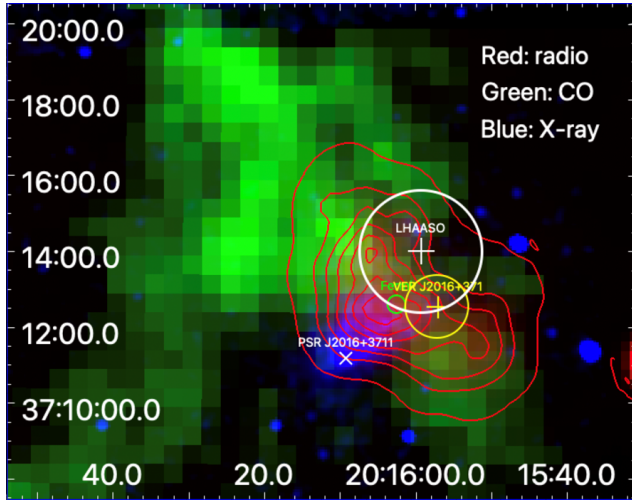


Figure 3: Tri-color image of CTB 87. “+” in white (yellow) marks the best-fit position of LHAASO (VERITAS) with 1sigma uncertainty. “X” represents the PSR found by FAST [13].

3. DISCUSSION

Time-dependent leptonic model: High-energy electrons injected from the pulsar wind nebula (PWN) upscatter cosmic microwave background (CMB) and infrared (IR) photons to very high-energy (VHE) ranges. The J2019+3649 region contains “young” electrons, while the J2021+3657 and J2018+3644 regions are dominated by “old” electrons that are injected at an earlier time.

For J2021+3657, we also explore a hadronic model due to its potential association with WR 141. Additionally, the star-forming region Sharpless 104 (Sh 2–104) may contribute a portion of the measured flux from J2018+3644. The hadronic emission model also works. As illustrated in Figure 2, the gas column density near J2018+3644 and J2021+3657 is derived from ^{12}CO line observations. However, for J2019+3649, the hadronic model does not work.

LHAASO J2016+3712 is linked to a point source coincident with the SNR CTB 87 with a TS value of 100.8 (corresponding to $\sim 10.0\sigma$). Analysis of data of Fermi in the 1 GeV - 1 TeV range revealed two point sources with distinct gamma-ray spectra [17]. A soft GeV spectrum (PsA: index 2.90) is typical of SNR shock-MC interactions, while the hard GeV spectrum of PsB (index 1.69) smoothly connects to the TeV spectrum, supporting PsB as the GeV counterpart of LHAASO J2016+3712 and VER J2016+371. Combining radio and X-ray observations of the PWN and the hard GeV spectrum characteristic of PWNe, we conclude that LHAASO J2016+3712 originates from the PWN associated with PSR J2016+3711.

4. Conclusions

In this work, we reanalyze the γ -ray emission from the LHAASO J2018+3651 region (1136.2 days of WCDA and 1064.9 days of KM2A data). Three new sources were detected during the LHAASO analysis, and the updated results for the three previously detected 1LHAASO sources indicate that a total of six source candidates were identified in this region. LHAASO J2018+3644, LHAASO J2021+3657, and LHAASO J2019+3649 are detected at a significance level exceeding

$20\sigma_{\text{local}}$, and their spectra are well-described by a power law with exponential cutoff. Those three sources are likely associated with PSR J2021+3651 and its X-ray pulsar wind nebula. Furthermore, LHAASO J2021+3651 may also be associated with WR 141. Additionally, LHAASO J2016+3712 is tentatively associated with the evolved supernova remnant CTB 87.

Acknowledgments

This work is supported by the following grants: the Department of Science and Technology of Sichuan Province, China (Nos. 2024ZYD0111), the National Key R&D program of China under the grant 2024YFA1611403. This research made use of the data from the Milky Way Imaging Scroll Painting (MWISP) project, which is a multi-line survey in 12CO/13CO/C18O along the northern galactic plane with PMO-13.7m telescope.

References

- [1] Abdo, A. A., Allen, B., Berley, D., et al. 2007, *Astrophys. J.*, 658, L33. <https://arxiv.org/abs/0611691>
- [2] Abdo, A. A., Abeysekara, U., Allen, B. T., et al. 2012, *Astrophys. J.*, 753, 159. <https://arxiv.org/abs/1202.0846>
- [3] Abeysekara, A. U., Archer, A., Aune, T., et al. 2018, *Astrophys. J.*, 861, 134, doi: [10.3847/1538-4357/aac4a2](https://doi.org/10.3847/1538-4357/aac4a2)
- [4] Abeysekara, A. U., Albert, A., Alfaro, R., et al. 2020, *Physical Review Letters*, 124, doi: [10.1103/PhysRevLett.124.021102](https://doi.org/10.1103/PhysRevLett.124.021102)
- [5] Aharonian, F., An, Q., Axikegu, et al. 2021, *Chinese Physics C*, 45, 085002, doi: [10.1088/1674-1137/ac041b](https://doi.org/10.1088/1674-1137/ac041b)
- [6] Aliu, E., Aune, T., Behera, B., et al. 2014, *Astrophys. J.*, 788, 78
- [7] Amenomori, M., Bao, Y. W., Bi, X. J., Chen, D., & Zhou, X. X. 2021, *Physical Review Letters*, 127
- [8] Cao, Z., Aharonian, F. A., An, Q., Axikegu, & Zuo, X. 2021, *Nature*, 594
- [9] Fang, J., Wen, L., Yu, H., & Chen, S. 2020, *Monthly Notices of the Royal Astronomical Society*, 498, 4901, doi: [10.1093/mnras/staa2703](https://doi.org/10.1093/mnras/staa2703)
- [10] Fleysher, R., Fleysher, L., Nemethy, P., Mincer, A. I., & Haines, T. J. 2004, *The Astrophysical Journal*, 603, 355, doi: [10.1086/381384](https://doi.org/10.1086/381384)
- [11] Halpern, J. P., Camilo, F., Giuliani, A., et al. 2008, , 688, L33, doi: [10.1086/594117](https://doi.org/10.1086/594117)
- [12] Hessels, J. W. T., Roberts, M. S. E., Ransom, S. M., et al. 2004, *The Astrophysical Journal*, 612

- [13] Liu, Q.-C., Zhong, W.-J., Chen, Y., et al. 2024, , 528, 6761, doi: [10.1093/mnras/stae351](https://doi.org/10.1093/mnras/stae351)
- [14] Moderksi, R., Sikora, M., Coppi, P. S., & Aharonian, F. A. 2005, Mon. Not. Roy. Astron. Soc., 364, 1488, doi: [10.1111/j.1365-2966.2005.09814.x](https://doi.org/10.1111/j.1365-2966.2005.09814.x), [10.1111/j.1365-2966.2005.09494.x](https://doi.org/10.1111/j.1365-2966.2005.09494.x)
- [15] Roberts, M. S. E., Hessels, J. W. T., Ransom, S. M., et al. 2002, *Astrophys. J.*, 577, L19
- [16] Sguera, V. 2008, in The 7th INTEGRAL Workshop, 82
- [17] Xin, Y., Tang, J., Ding, W., et al. 2025, , 981, 33, doi: [10.3847/1538-4357/adb282](https://doi.org/10.3847/1538-4357/adb282)

Zhen Cao^{1,2,3}, F. Aharonian^{3,4,5,6}, Y.X. Bai^{1,3}, Y.W. Bao⁷, D. Bastieri⁸, X.J. Bi^{1,2,3}, Y.J. Bi^{1,3}, W. Bian⁷, A.V. Bukevich⁹, C.M. Cai¹⁰, W.Y. Cao⁴, Zhe Cao^{11,4}, J. Chang¹², J.F. Chang^{1,3,11}, A.M. Chen⁷, E.S. Chen^{1,3}, H.X. Chen¹³, Liang Chen¹⁴, Long Chen¹⁰, M.J. Chen^{1,3}, M.L. Chen^{1,3,11}, Q.H. Chen¹⁰, S. Chen¹⁵, S.H. Chen^{1,2,3}, S.Z. Chen^{1,3}, T.L. Chen¹⁶, X.B. Chen¹⁷, X.J. Chen¹⁰, Y. Chen¹⁷, N. Cheng^{1,3}, Y.D. Cheng^{1,2,3}, M.C. Chu¹⁸, M.Y. Cui¹², S.W. Cui¹⁹, X.H. Cui²⁰, Y.D. Cui²¹, B.Z. Dai¹⁵, H.L. Dai^{1,3,11}, Z.G. Dai⁴, Danzengluobu¹⁶, Y.X. Diao¹⁰, X.Q. Dong^{1,2,3}, K.K. Duan¹², J.H. Fan⁸, Y.Z. Fan¹², J. Fang¹⁵, J.H. Fang¹³, K. Fang^{1,3}, C.F. Feng²², H. Feng¹, L. Feng¹², S.H. Feng^{1,3}, X.T. Feng²², Y. Feng¹³, Y.L. Feng¹⁶, S. Gabici²³, B. Gao^{1,3}, C.D. Gao²², Q. Gao¹⁶, W. Gao^{1,3}, W.K. Gao^{1,2,3}, M.M. Ge¹⁵, T.T. Ge²¹, L.S. Geng^{1,3}, G. Giacinti⁷, G.H. Gong²⁴, Q.B. Gou^{1,3}, M.H. Gu^{1,3,11}, F.L. Guo¹⁴, J. Guo²⁴, X.L. Guo¹⁰, Y.Q. Guo^{1,3}, Y.Y. Guo¹², Y.A. Han²⁵, O.A. Hannuksela¹⁸, M. Hasan^{1,2,3}, H.H. He^{1,2,3}, H.N. He¹², J.Y. He¹², X.Y. He¹², Y. He¹⁰, S. Hernández-Cadena⁷, Y.K. Hor²¹, B.W. Hou^{1,2,3}, C. Hou^{1,3}, X. Hou²⁶, H.B. Hu^{1,2,3}, S.C. Hu^{1,3,27}, C. Huang¹⁷, D.H. Huang¹⁰, J.J. Huang^{1,2,3}, T.Q. Huang^{1,3}, W.J. Huang²¹, X.T. Huang²², X.Y. Huang¹², Y. Huang^{1,3,27}, Y.Y. Huang¹⁷, X.L. Ji^{1,3,11}, H.Y. Jia¹⁰, K. Jia²², H.B. Jiang^{1,3}, K. Jiang^{11,4}, X.W. Jiang^{1,3}, Z.J. Jiang¹⁵, M. Jin¹⁰, S. Kaci⁷, M.M. Kang²⁸, I. Karpikov⁹, D. Khangulyan^{1,3}, D. Kuleshov⁹, K. Kurinov⁹, B.B. Li¹⁹, Cheng Li^{11,4}, Cong Li^{1,3}, D. Li^{1,2,3}, F. Li^{1,3,11}, H.B. Li^{1,2,3}, H.C. Li^{1,3}, Jian Li⁴, Jie Li^{1,3,11}, K. Li^{1,3}, L. Li²⁹, R.L. Li¹², S.D. Li^{14,2}, T.Y. Li⁷, W.L. Li⁷, X.R. Li^{1,3}, Xin Li^{11,4}, Y.Z. Li^{1,2,3}, Zhe Li^{1,3}, Zhuo Li³⁰, E.W. Liang³¹, Y.F. Liang³¹, S.J. Lin²¹, B. Liu⁴, C. Liu^{1,3}, D. Liu²², D.B. Liu⁷, H. Liu¹⁰, H.D. Liu²⁵, J. Liu^{1,3}, J.L. Liu^{1,3}, J.R. Liu¹⁰, M.Y. Liu¹⁶, R.Y. Liu¹⁷, S.M. Liu¹⁰, W. Liu^{1,3}, X. Liu¹⁰, Y. Liu⁸, Y. Liu¹⁰, Y.N. Liu²⁴, Y.Q. Lou²⁴, Q. Luo²¹, Y. Luo⁷, H.K. Lv^{1,3}, B.Q. Ma^{25,30}, L.L. Ma^{1,3}, X.H. Ma^{1,3}, J.R. Mao²⁶, Z. Min^{1,3}, W. Mitthumsiri³², G.B. Mou³³, H.J. Mu²⁵, Y.C. Nan^{1,3}, A. Neronov²³, K.C.Y. Ng¹⁸, M.Y. Ni¹², L. Nie¹⁰, L.J. Ou⁸, P. Pattarakijwanich³², Z.Y. Pei⁸, J.C. Qi^{1,2,3}, M.Y. Qi^{1,3}, J.J. Qin⁴, A. Raza^{1,2,3}, C.Y. Ren¹², D. Ruffolo³², A. Sáiz³², M. Saeed^{1,2,3}, D. Semikoz²³, L. Shao¹⁹, O. Shchegolev^{9,34}, Y.Z. Shen¹⁷, X.D. Sheng^{1,3}, Z.D. Shi⁴, F.W. Shu²⁹, H.C. Song³⁰, Yu.V. Stenkin^{9,34}, V. Stepanov⁹, Y. Su¹², D.X. Sun^{4,12}, H. Sun²², Q.N. Sun^{1,3}, X.N. Sun³¹, Z.B. Sun³⁵, N.H. Tabasam²², J. Takata³⁶, P.H.T. Tam²¹, H.B. Tan¹⁷, Q.W. Tang²⁹, R. Tang⁷, Z.B. Tang^{11,4}, W.W. Tian^{2,20}, C.N. Tong¹⁷, L.H. Wan²¹, C. Wang³⁵, G.W. Wang⁴, H.G. Wang⁸, H.H. Wang²¹, J.C. Wang²⁶, K. Wang³⁰, Kai Wang¹⁷, Kai Wang³⁶, L.P. Wang^{1,2,3}, L.Y. Wang^{1,3}, L.Y. Wang¹⁹, R. Wang²², W. Wang²¹, X.G. Wang³¹, X.J. Wang¹⁰, X.Y. Wang¹⁷, Y. Wang¹⁰, Y.D. Wang^{1,3}, Z.H. Wang²⁸, Z.X. Wang¹⁵, Zheng Wang^{1,3,11}, D.M. Wei¹², J.J. Wei¹², Y.J. Wei^{1,2,3}, T. Wen¹⁵, S.S. Weng³³, C.Y. Wu^{1,3}, H.R. Wu^{1,3}, Q.W. Wu³⁶, S. Wu^{1,3}, X.F. Wu¹², Y.S. Wu⁴, S.Q. Xi^{1,3}, J. Xia^{4,12}, J.J. Xia¹⁰, G.M. Xiang^{14,2}, D.X. Xiao¹⁹, G. Xiao^{1,3}, Y.L. Xin¹⁰, Y. Xing¹⁴, D.R. Xiong²⁶, Z. Xiong^{1,2,3}, D.L. Xu⁷, R.F. Xu^{1,2,3}, R.X. Xu³⁰, W.L. Xu²⁸, L. Xue²², D.H. Yan¹⁵, J.Z. Yan¹², T. Yan^{1,3}, C.W. Yang²⁸, C.Y. Yang²⁶, F.F. Yang^{1,3,11}, L.L. Yang²¹, M.J. Yang^{1,3}, R.Z. Yang⁴, W.X. Yang⁸, Y.H. Yao^{1,3}, Z.G. Yao^{1,3}, X.A. Ye¹², L.Q. Yin^{1,3}, N. Yin²², X.H. You^{1,3}, Z.Y. You^{1,3}, Y.H. Yu⁴, Q. Yuan¹², H. Yue^{1,2,3}, H.D. Zeng¹², T.X. Zeng^{1,3,11}, W. Zeng¹⁵, M. Zha^{1,3}, B.B. Zhang¹⁷, B.T. Zhang^{1,3}, F. Zhang¹⁰, H. Zhang⁷, H.M. Zhang³¹, H.Y. Zhang¹⁵, J.L. Zhang²⁰, Li Zhang¹⁵, P.F. Zhang¹⁵, P.P. Zhang^{4,12}, R. Zhang¹², S.R. Zhang¹⁹, S.S. Zhang^{1,3}, W.Y. Zhang¹⁹, X. Zhang³³, X.P. Zhang^{1,3}, Yi Zhang^{1,12}, Yong Zhang^{1,3}, Z.P. Zhang⁴, J. Zhao^{1,3}, L. Zhao^{11,4}, L.Z. Zhao¹⁹, S.P. Zhao¹², X.H. Zhao²⁶, Z.H. Zhao⁴, F. Zheng³⁵, W.J. Zhong¹⁷, B. Zhou^{1,3}, H. Zhou⁷, J.N. Zhou¹⁴, M. Zhou²⁹, P. Zhou¹⁷, R. Zhou²⁸, X.X. Zhou^{1,2,3}, X.X. Zhou¹⁰, B.Y. Zhu^{4,12}, C.G. Zhu²², F.R. Zhu¹⁰, H. Zhu²⁰, K.J. Zhu^{1,2,3,11}, Y.C. Zou³⁶, X. Zuo^{1,3}

¹ Key Laboratory of Particle Astrophysics & Experimental Physics Division & Computing Center, Institute of High Energy Physics, Chinese Academy of Sciences, 100049 Beijing, China

² University of Chinese Academy of Sciences, 100049 Beijing, China

³ TIANFU Cosmic Ray Research Center, Chengdu, Sichuan, China

⁴ University of Science and Technology of China, 230026 Hefei, Anhui, China

⁵ Yerevan State University, 1 Alek Manukyan Street, Yerevan 0025, Armenia

⁶ Max-Planck-Institut for Nuclear Physics, P.O. Box 103980, 69029 Heidelberg, Germany

⁷ Tsung-Dao Lee Institute & School of Physics and Astronomy, Shanghai Jiao Tong University, 200240 Shanghai, China

⁸ Center for Astrophysics, Guangzhou University, 510006 Guangzhou, Guangdong, China

⁹ Institute for Nuclear Research of Russian Academy of Sciences, 117312 Moscow, Russia

¹⁰ School of Physical Science and Technology & School of Information Science and Technology, Southwest Jiaotong University, 610031 Chengdu, Sichuan, China

¹¹ State Key Laboratory of Particle Detection and Electronics, China

¹² Key Laboratory of Dark Matter and Space Astronomy & Key Laboratory of Radio Astronomy, Purple Mountain Observatory, Chinese Academy of Sciences, 210023 Nanjing, Jiangsu, China

¹³ Research Center for Astronomical Computing, Zhejiang Laboratory, 311121 Hangzhou, Zhejiang, China

¹⁴ Shanghai Astronomical Observatory, Chinese Academy of Sciences, 200030 Shanghai, China

¹⁵ School of Physics and Astronomy, Yunnan University, 650091 Kunming, Yunnan, China

¹⁶ Key Laboratory of Cosmic Rays (Tibet University), Ministry of Education, 850000 Lhasa, Tibet, China

¹⁷ School of Astronomy and Space Science, Nanjing University, 210023 Nanjing, Jiangsu, China

¹⁸ Department of Physics, The Chinese University of Hong Kong, Shatin, New Territories, Hong Kong, China

¹⁹ Hebei Normal University, 050024 Shijiazhuang, Hebei, China

²⁰ Key Laboratory of Radio Astronomy and Technology, National Astronomical Observatories, Chinese Academy of Sciences, 100101 Beijing, China

²¹ School of Physics and Astronomy (Zhuhai) & School of Physics (Guangzhou) & Sino-French Institute of Nuclear Engineering and Technology (Zhuhai), Sun Yat-sen University, 519000 Zhuhai & 510275 Guangzhou, Guangdong, China

²² Institute of Frontier and Interdisciplinary Science, Shandong University, 266237 Qingdao, Shandong, China

²³ APC, Université Paris Cité, CNRS/IN2P3, CEA/IRFU, Observatoire de Paris, 119 75205 Paris, France

²⁴ Department of Engineering Physics & Department of Physics & Department of Astronomy, Tsinghua University, 100084 Beijing, China

²⁵ School of Physics and Microelectronics, Zhengzhou University, 450001 Zhengzhou, Henan, China

²⁶ Yunnan Observatories, Chinese Academy of Sciences, 650216 Kunming, Yunnan, China

²⁷ China Center of Advanced Science and Technology, Beijing 100190, China

²⁸ College of Physics, Sichuan University, 610065 Chengdu, Sichuan, China

²⁹ Center for Relativistic Astrophysics and High Energy Physics, School of Physics and Materials

Science & Institute of Space Science and Technology, Nanchang University, 330031 Nanchang, Jiangxi, China

³⁰ School of Physics & Kavli Institute for Astronomy and Astrophysics, Peking University, 100871 Beijing, China

³¹ Guangxi Key Laboratory for Relativistic Astrophysics, School of Physical Science and Technology, Guangxi University, 530004 Nanning, Guangxi, China

³² Department of Physics, Faculty of Science, Mahidol University, Bangkok 10400, Thailand

³³ School of Physics and Technology, Nanjing Normal University, 210023 Nanjing, Jiangsu, China

³⁴ Moscow Institute of Physics and Technology, 141700 Moscow, Russia

³⁵ National Space Science Center, Chinese Academy of Sciences, 100190 Beijing, China

³⁶ School of Physics, Huazhong University of Science and Technology, Wuhan 430074, Hubei, China